Parallel Operation of Battery Chargers in Small Satellite Electrical Power Systems

Mallikarjun Kompella, R. Sudharshan Kaarthik, H. Priyadarshnam, and Harsha Simha M.S.
Department of Avionics, Indian Institute of Space Science and Technology, Thiruvananthapuram, India.
vlnmallikarjunkompella@gmail.com

***Abstract*—CubeSats are a class of nano-satellites primarily built using commercial off-the-shelf components for electronics and structure, aimed at space and atmospheric research. The Electrical Power System (EPS) of the CubeSat is responsible for extracting power from solar panels to provide regulated power to all the satellite subsystems and using the surplus power to charge the satellite's batteries in order to sustain the satellite's operations during eclipses. The battery charger integrated circuit, with the photovoltaic (PV) input, should be able to charge the batteries of the satellite while extracting maximum power from the solar panels. Since there are multiple solar panels for a given satellite, the chosen charging scheme should be able to operate in parallel from different PV inputs and common battery output terminals. This manuscript describes parallel operation of a PV battery charger, which is capable of interfacing PV panels of different incident solar radiation with a common battery. Experimental results are presented to validate the circuit operation.**

***Index Terms*—Small satellite, parallel converters, maximum power point, battery charging, solar panel, load sharing.**

I. INTRODUCTION

A CubeSat is a type of miniaturized satellite for space research made up of multiple units of $10\,\text{cm}\times10\,\text{cm}\times11.35\,\text{cm}$ with a maximum mass of $1.33\,\text{kg}$. The primary objective of CubeSats is to provide access to space for small payloads from universities across the globe [1]. CubeSats now provide a cost effective platform for scientific investigations, new technology demonstrations and advanced mission concepts [2].

The Electrical Power System (EPS) of a CubeSat has the following functions: (i) extract solar power from solar panels to supply power to the loads of the satellite, (ii) use the excess power to charge the satellite batteries, (iii) to sense and communicate voltage, current and temperature data to the On-board Computer (OBC) for health monitoring and telemetry, (iv) cutoff power to the whole satellite before deployment from the launch vehicle, (v) to maintain the battery's State of Charge (SoC) and temperature within the recommended limits of operation, and (vi) to selectively cutoff power to different subsystems of the satellite.

For a typical CubeSat, the PV panels are placed on different sides of the CubeSat surfaces as shown in Fig. 1. This means that there are multiple solar panels with different irradiation levels (because of different orientation) and hence will be functioning at different operating points.

The function of the PV battery charger circuit is to charge the batteries, which requires its coordinated operation in parallel configuration while maintaining the individual panels at Maximum Power Point (MPP) of respective I–V curves.

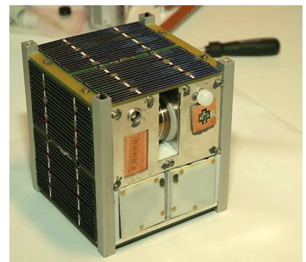

Fig. 1: An image showing PV panels on different sides of a CubeSat.

This manuscript proposes a circuit which can work in parallel configuration from different PV inputs, in two different types of load connection topologies, (i) source-fed, and (ii) battery-fed connections.

II. OVERALL ARCHITECTURE OF CUBESAT EPS

The proposed satellite EPS architecture can be divided into two parts as shown in Fig. 2. They are 1) Source side, and 2) Load side. The source side consists of electric circuits to charge the batteries. The load side is responsible for regulating the received surplus power from source side and batteries to desired voltage and current levels to provide the same to the satellite loads.

It can be noted that in Fig. 2, the kill switch-1 is used to turn off power to the whole satellite before deployment from the launch vehicle, and kill switch-2 is used to prevent the discharge of the battery during the assembly, integration and pre-launch operations of the satellite.

The voltage and current sensors sense the operating voltage and current consumption of different subsystems. The Analog-to-Digital converter is used to convert the analog temperature data to digital signals which are sent to On-board Computer(OBC) via a suitable communication interface. The fuel gauge measures the battery's voltage and estimates the battery's State of Charge(SoC) which are communicated to OBC. The satellite loads can be individually powered off by disabling the enable pins of corresponding power regulators by the OBC.

III. PARALLEL OPERATION OF CHARGER CIRCUITS

Often, a CubeSat has more than one solar panel which requires the source side of the EPS to operate from different solar panel inputs at different operating points and a common

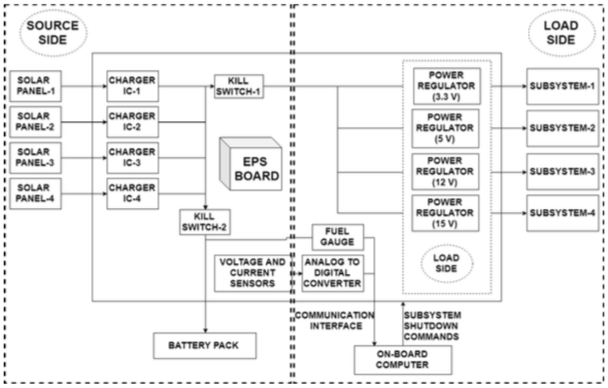

Fig. 2: Architecture of CubeSat EPS.

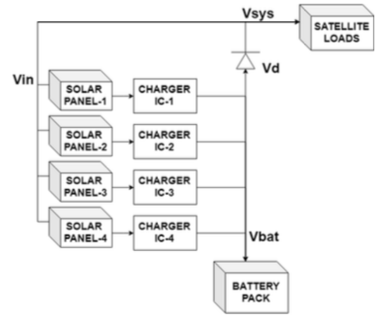

Fig. 3: Source-fed load connection topology in CubeSat EPS.

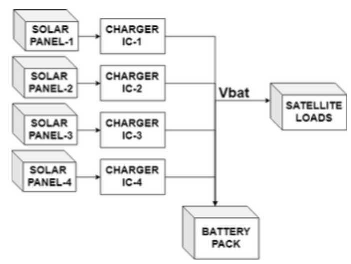

Fig. 4: Battery-fed load connection topology CubeSat EPS.

battery output terminals. In this section, the parallel operation of two converters is demonstrated.

A mid-power Li-ion battery charger based on buck converter topology is designed for AHAN, the small satellite mission of Indian Institute of Space Science and Technology. It can provide a maximum charge current output of up to 2 A using the Constant Current – Constant Voltage (CC-CV) charging algorithm while maintaining the solar panel input at Maximum Power Point (MPP) using Input Voltage Regulation Loop. Batteries of float voltages up to 14.4 V can be charged; the float voltage is programmed by a resistor divider on the output side of the converter [3].

With respect to the way the satellite loads are connected to the source side of EPS, there are two load connection topologies namely 1) Source-fed topology and 2) Battery-fed topology.

A. Source-fed topology

In this topology, the load is connected to the solar panels and the battery through a Diode-ORing technique. Under certain operating conditions, this topology may result in sub-optimal usage of input solar power. Consider the source-fed topology shown in Fig. 4. If the system load increases beyond the current capability of the input solar panel, then the diode between the system load and the battery starts conducting to support this high load. Under such conditions, V_{sys} (voltage at the system load node) and V_{in} (solar panel voltage) become V_{bat} (battery voltage), making the IC lose control of the solar panel operating voltage. Operation of solar panels at a voltage other than its maximum power point voltage results in sub-optimal usage of power from solar panels. So for this topology, the solar panel should be sized such that, on average, its power capacity is greater than the average load power [4].

Case 1: During battery charging, diode does not conduct. Hence

$$V_{in} = V_{sys} \tag{1}$$

Case 2: When load increases beyond panel current capability, battery discharges through the diode. Hence

$$V_{in} = V_{sys} = V_{bat} - V_d \tag{2}$$

B. Battery-fed topology

In this topology, the load is connected in parallel to the battery and the output of parallel configuration of charger circuits as shown in the Fig. 5, which makes the charger circuit to always maintain complete control of the solar panel operating conditions. If the system load exceeds the programmed charge current, then the battery discharges to supply the additional current required for the load. The advantage of this topology is that it maximizes the power combination of both battery and system load. The trade-offs involved in this topology are non-availability of power to system load as soon as the input power is available in case of a heavily discharged battery and difficulty in differentiating between the charge current and system load current which impacts the charge termination algorithms. There is also a chance of permanent damage to the battery if a system load can discharge the battery below the pre-charge threshold of charger circuit and that same load exceeds the pre-charge current, it is possible that the battery will be further drained even with an input supply present, permanently damaging the battery [5].

C. Operation under various illuminations

As shown in Fig. 6, a solar cell exhibits a unique property of negligible variation of voltage MPP under varying illuminations, which allows the designed architecture to extend its operating range into various illumination conditions. The designed architecture makes use of this property to set the MPP as a fixed point using passive components such as resistors, as will be described in the next section.

Authorized licensed use limited to: Indian Institute of Technology Patna. Downloaded on September 02,2025 at 08:05:17 UTC from IEEE Xplore. Restrictions apply.

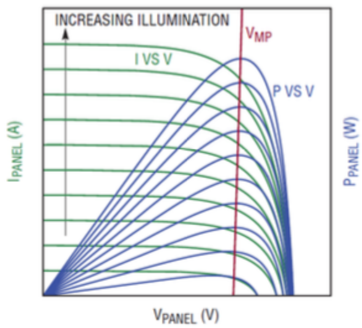

Fig. 5: Variation of solar cell I–V curve under different illuminations.

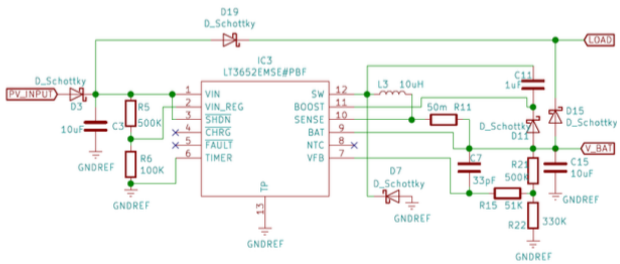

Fig. 6: Schematic of one converter on source-side in source-fed topology.

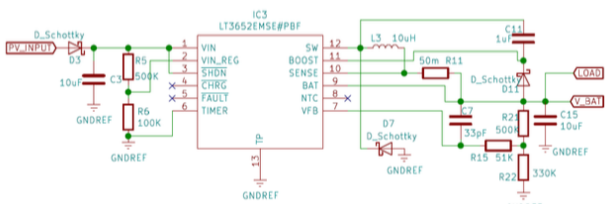

Fig. 7: Schematic of one converter on source-side in battery-fed topology.

IV. Schematics of the Design

A. Source-side circuit schematics

Fig. 7 and Fig. 8 show the schematics of the battery charging converter that is connected to a single PV panel in source-fed topology and battery-fed topology respectively. R5 and R6 determine the input MPPT set point (16.2 V for this design). R21 and R22 determine the battery's float voltage (8.3 V for this design). R11 determines the maximum charge current (2 A in this design). Datasheet instructions are followed to determine the values.

V. Transient and Steady-State Simulation Results

The designed EPS architecture is simulated in LTSPICE to validate the architecture with three charger circuits in parallel. The battery voltage, charge current output from one charger and total charge current output from the three chargers in parallel are shown in Fig. 9.

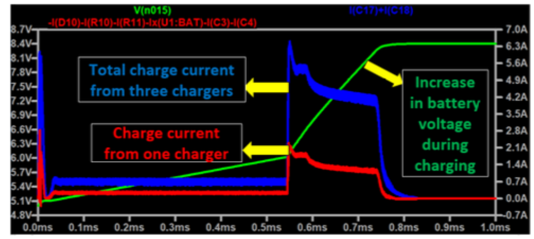

Fig. 8: Simulation results of designed architecture.

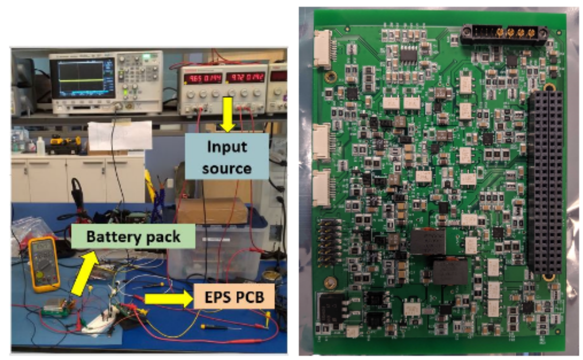

(a) (b)

Fig. 9: (a) Experimental setup; (b) PCB of the satellite EPS.

TABLE I: Test results of battery charging circuit

S.No	PV-1 Voltage/Current	PV-2 Voltage/Current	Charge current
1.	10.01 V / 0.999 A	9.63 V / 0.501 A	0.555 A
2.	0 V / 0 A	8.26 V / 0.501 A	-0.607 A
3.	0 V / 0 A	0 V / 0 A	-1.201 A

VI. Experimental Results

The circuit based on architecture shown in Fig. 2 has been designed in battery-fed topology. Schematics and Layout have been implemented in KiCAD. The PCB was fabricated and functional tests were conducted as shown in Fig. **??**.

For testing purposes, two channels are used to demonstrate the parallel operation. The voltage and current readings of two different input primary sources taken from a solar panel simulator and battery charge current readings are taken in different modes (Table I) and inferences are as stated below.

VII. Conclusion

The developed circuit is a part of the AHAN mission, the first small satellite mission of Indian Institute of Space Science and Technology. Preliminary experimental results, details of the architecture, schematics and test setup have been provided. The parallel operation of designed converters is tested successfully in source-fed and battery-fed load connection topologies.

Authorized licensed use limited to: Indian Institute of Technology Patna. Downloaded on September 02,2025 at 08:05:17 UTC from IEEE Xplore. Restrictions apply.

Acknowledgment

The authors would like to acknowledge the AHAN project team (optional).

References

[1] A. Hutputtanasin and A. Toorian, ”CubeSat Design Specification”, May 15, 2005.
[2] E. Mabrouk, ”What are SmallSats and CubeSats”, NASA, Aug. 7, 2017.
[3] J. Drew, ”Designing a Solar Cell Battery Charger”, Linear Technology Magazine, Dec. 2009.
[4] T. Barcelo, ”Multi-Chemistry Battery Charger Supports Maximum Power Point Tracking for Solar Panels”, LT Journal of Analog Innovation, Apr. 2017.
[5] J. Celani, ”Solar Battery Charger Maintains High Efficiency in Low Light”, LT Journal of Analog Innovation, Oct. 2013.

Authorized licensed use limited to: Indian Institute of Technology Patna. Downloaded on September 02,2025 at 08:05:17 UTC from IEEE Xplore. Restrictions apply.